



Pre-conceptual design of an encapsulated breeder commercial blanket for the STEP fusion reactor

J. Fradera ^{*,1,a}, S. Sádaba ^{a,1,a}, F. Calvo ^a, S. Ha ^b, S. Merriman ^b, P. Gordillo ^c, J. Connell ^c, A. Elfaraskoury ^a, B. Echeveste ^a

^a IDOM, No 1 St Ann Street M2 7LR, Manchester, United Kingdom

^b UKAEA, Culham Science Centre, Abingdon, Oxfordshire, OX14 3DB, United Kingdom

^c Nuclear AMRC, University of Sheffield, Advanced Manufacturing Park, Brunel Way, Rotherham, S60 5WG, United Kingdom

ARTICLE INFO

Keywords:

Fusion
STEP
Breeding blanket
Encapsulated fuel
Tritium
Self-sufficiency
Thermal-hydraulics
Mechanical
Neutronics
FLiBe

ABSTRACT

As part of the UKAEA Spherical Tokamak for Energy Production (STEP) fusion power station programme, a novel breeding blanket design was assessed. A conceptual design of STEP, which will be an innovative plan for a commercially-viable fusion power station, will be completed by 2024. The final aim of the current assessment is to find a pre-conceptual design that can be manufactured with existing techniques without compromising the fuel self-sufficiency, the heat removal and the shielding functions. The proposed concept, an starting point towards a commercial blanket design, is based on encapsulating the breeding material into hollow spheres forming a gas cooled packed bed. The generated tritium in the breeding material, as well as helium, will be extracted from the pebbles and directly removed from the blanket by the cooling gas. A frontal multiplier as well as a back reflector have also been studied to maximize the tritium generation. This paper, which is a decided first step towards a breeding blanket for STEP, covers the material design properties and their compatibility, the design configuration, the neutronics analysis, the thermal-hydraulics analysis, a preliminary structural analysis, safety aspects and waste segregation and disposal.

1. Introduction

The United Kingdom Atomic Energy Agency (UKAEA) Spherical Tokamak for Energy Production (STEP) is an innovative plan for a commercially-viable fusion power station. A conceptual design of the reactor is foreseen to be completed by 2024. Within this ambitious programme, one of the key components to be developed is the Breeding Blanket (BB), which provides shielding from plasma fusion neutrons, extracts heat for power generation and breeds tritium (T) to achieve the self-sufficiency principle. This work presents a pre-conceptual design of a possible BB for STEP focusing on the mentioned blanket functions and especially on the manufacturability with available techniques and existing materials. The work aims to be a first step of many in a design process towards a working blanket.

It must be noted that the assessment has focused on a commercial BB concept, so a balance between high performance materials, commercially available and reduced cost materials has been sought. Despite of the mentioned compromise to focus on a commercial BB, the presented

concept allows different breeding materials, even exotic ones, to be used and aims to ensure self-sufficiency, safety and a high thermal efficiency for a high volumetric power density.

A series of sensitivity analyses (see Section 4) have been carried out to both assess the feasibility and the performance of the proposed concept and to improve the layout. This paper exposes the pre-conceptual design excluding any optimization of the blanket dimensions. Results include a significant uncertainty that will be cleared in future stages of the design process. The final aim is to narrow the design space, detect and overcome stoppers, resulting in a feasible design start point.

2. State of the art and concept overview

The applied methodology for the design of the encapsulated BB concept is based on an analysis of previous blanket concepts, a series of constraints intrinsic to the blanket functions and on splitting the functions of the blanket. In addition, lessons learned from other blanket projects have been implemented.

* Corresponding author.

E-mail addresses: jorge.fradera@idom.com (J. Fradera), samuel.ha@ukaea.uk (S. Ha), pablo.gordillo@namrc.co.uk (P. Gordillo).

¹ Both authors have contributed equally to this work.

Glossary*Abbreviations*

NAMRC	Nuclear Advanced Manufacturing Research Centre
BB	Breeding Blanket
BC	Boundary Condition
BU	Breeder Unit
CFD	Computational Fluid Dynamics
DCLL	Dual Coolant Lithium Lead
EBW	Electron Beam Welding
FW	First Wall
HCLL	Helium Cooled Lithium Lead
HCPB	Helium Cooled Packed Bed
HT	High temperature (above 450 C for Eurofer 97)
HTC	Heat transfer coefficient
IPFL	Immediate Plastic Flow Localization
LT	Low temperature (below 450 C for Eurofer 97)
MCNP	Monte Carlo N-Particle
MHD	Magneto Hydro Dynamics
NHD	Nuclear Heat Deposition
NDT	Non-Destructive Tests

STEP	Spherical Tokamak for Energy Production
TBR	Tritium Breeding Ratio
UKAEA	United Kingdom Atomic Energy Agency
VOF	Volume of Fluid
V	Fatigue usage fraction

Greek characters

ϵ	void fraction
ϕ	Neutron flux

Latin characters

e	FLiBe fraction
D	deuterium
H	nuclear heat deposition
H	protium
TF	tritium fluoride
T	temperature
T	tritium

Subscripts

x, y, z	coordinates
-----------	-------------

Previous blanket concepts can be divided into two main categories: liquid breeders, e.g. the Helium Cooled Lithium Lead (HCLL) [1] and the Dual Coolant Lithium LEad (DCLL) [2], and solid breeders, e.g. the Helium Cooled Pebble Bed (HCPB) [3] among many others. The present design can be understood as a hybrid between both categories where features from each technology, i.e., the pebble bed form the HCPB and 2 LiF - BeF₂ (FLiBe) from Dual Coolant Molten Salt Blanket, or Arc Blanket (see e.g. [4] among others), has been implemented.

Shielding from plasma (~ 14MeV) neutrons function is distributed among the multiplier, the structural material, the breeder material and the reflector.

The heat extraction function is carried out by a gas flowing through the pebble bed like in the HCPB concept. Pumping requirements and heat transfer capabilities involve pressurized gas coolants. Therefore, the blanket shall include pressure components that can be easily manufactured, installed, welded and inspected.

Tritium production function is achieved by means of the $\text{Li}^{6(n,\alpha)\text{H}^3}$ and $\text{Li}^{7(n,n'\alpha)\text{H}^3}$ reactions. As far as the authors know, in all blanket concepts the generated T diffuses through the breeder material and eventually degasses as T₂. On one hand, solid breeder blanket concepts usually accumulate T in the breeding material which may become an issue from the safety point of view (see [5] and references therein). Furthermore, He is generated at a similar rate as T, so nucleation is expected resulting in material swelling. On the other hand, liquid breeder blanket concepts usually have low T solubilities [6], so extracting T is more efficient and no swelling is expected in the breeder material. However, He may eventually nucleates and accumulate in the cooling system (see, e.g., [7–9]). Note that He nucleation has only been evaluated by means of simulation tools, so the actual impact on the system must be evaluated experimentally in order to verify its impact (T accumulation in gas pockets and heat transfer reduction).

The proposed blanket decouples the heat extraction function from the breeding one by allowing gases to flow through as the breeder is encapsulated in a pebble. Note that other solid breeder concepts use small bare or coated pebbles. In the presented concept, the pebbles are much larger (1-3cm) and no coating is used but a solid independent body ceramic shell inside a metallic jail. As opposed to solid breeders, in the present concept the breeder material is a liquid, removing or mitigating the He issue. The jail is used to give the pebble bed structural integrity without removing the heat extraction capability.

The neutron multiplier function, needed to achieve high Tritium

Breeding Ratios (TBR), has been partially or totally decoupled from the breeding and cooling functions by placing the multiplier material outside the pipes that hold the pebble bed. It must be noted that this decoupling implies the use of materials that are vacuum compatible and do not degas neither T, nor He. Note also that if FLiBe is used as breeder, the multiplication effect is coupled to the breeding function inside the pebble. Then, in this case, the T generation through $\text{Be}^9(n,2n)\text{Li}^7$ follows the same extraction path as for Li. It must be noted that other concepts using FLiBe exists like the Dual Coolant Molten Salt Blanket, the immersed blanket concept and some concepts for Inertial Confinement Fusion reactors (ICF) (see among others [4],[10],[11]).

Once the blanket functions were decoupled as much as possible, a series of sensitivity analyses were performed to assess each function separately.

3. Blanket configuration

The present section exposes the blanket pre-conceptual design configuration as well as the selection of candidate materials.

The proposed blanket is based on encapsulating the breeder into pebbles of a gas cooled packed bed. A top and bottom manifolds connected by vertical pipes allow the packed bed cooling by means of a gas. A frontal multiplier together with a multiplier pebble bed among the pipes and a back reflector are implemented to improve the neutron economy and allow TBRs > 1.

It must be highlighted that the present blanket concept is being developed for the STEP reactor, which will be a spherical TOKAMAK. However, as the STEP design is not fully completed and many parameters are still unknown, this spherical configuration will not be accounted for. A planar blanket will be assumed. Note also that the presented concept could be applied to other fusion reactor geometries.

3.1. Encapsulated breeder

As has already been mentioned, several breeders can be used (see e.g. [12]) with the proposed design with very little modifications as the material is encapsulated inside a pebble. For the present work FLiBe (Li₂-BeF₄) [13] has been selected as the breeder material. Note that other blanket concepts that use this molten salt exist, e.g., the ARC reactor [14] or the US APEX programme [15]. FLiBe has a high TBR and neutron multiplication capability close to liquid breeders like Pb₁₇Li₈₃

as exposed in [16] and references therein. FLiBe has a X-eutectic, with 0.328% Be and a melting temperature of 458.9°C, and an eutectic, with 0.531% Be and a melting temperature of 363.5°C. The highest the Be concentration the lowest the viscosity, which is a critical parameter regarding the thermal-hydraulics of a liquid breeder blanket. For the presented concept, as the FLiBe will be encapsulated, the viscosity may only affect the He nucleation onset with very little impact on the behaviour of the T extraction. Note that T transport in FLiBe systems is rather complex as shown in Fig. 1. However, a low melting temperature is preferred to work in the temperature window of the structural materials. Therefore, if a high Li content is used, the pebbles will have to be thermally isolated and withstand temperatures above the structural material limit. Alternative breeders in [17] include LiF-LiI-LiCl molten salts, with triple eutectic points down to 340°C.

The generated T and He in the FLiBe will eventually nucleate generating a gas pocket. To enhance this process the pebbles are designed so a coolant gas pocket is included in the pebble. Therefore, both T and He will degas to the pocket after diffusion or nucleation.

The decoupling of the cooling from the breeding function and the adoption of a pebble rises the following issues:

- T and He extraction from the pebble.
- FLiBe operating temperature window.
- FLiBe material compatibility.
- Pebble shell operating temperature window.
- Pebble heat removal.

The T extraction can be achieved either by diffusion through a metallic shell or by porous diffusion through, e.g., a ceramic one. The former is a slow process that can be limited by surface phenomena and the latter involves a pore size small enough to prevent FLiBe leakage. When He generation is accounted for, the porous shell solution becomes the only viable option. Otherwise He will accumulate and pressure build-up will eventually lead to an structural integrity problem or it will force the blanket to be removed from the reactor.

Regarding the FLiBe operating temperature, the porous shell, made, e.g., of a ceramic material like Silica, porous graphite or SiC, will have a

lower conductivity than that of a metallic shell, so it can be used to increase the operating temperature window of the FLiBe.

FLiBe is known to corrode structural materials, especially if T is generated. Dissolved hydrogen, or any of its isotopes, in FLiBe exists in atomic form. A RedOx reaction between T and F determines the existence of TF, which is very corrosive. If TF exists in the FLiBe it can corrode a metallic shell or it can be extracted along with T and He to the coolant stream posing a major problem to the primary coolant circuit. In both cases the generation of TF must be prevented. A small amount of metallic Be can shift the RedOx reaction so T is desorbed in its molecular form T₂. Other metals like Zr could be used as RedOx controllers, but then activation might become a problem.

The use of a porous shell comes not only with a structural problem, but also with a dust generation issue. The present concept uses a metallic jail made of structural material around the porous shell to prevent the contact among pebbles, withstand the weight of the packed bed and allow deformations due to mechanical loads. This jail poses no significant impact on the extraction or cooling of the pebbles.

The pebble design is as follows:

- Molten FLiBe as breeding material.
- Metallic Be as RedOx controller to prevent the generation of TF.
- A coolant gas pocket to allow pressure changes and, T and He degassing.
- A ceramic porous shell that allows T and He extraction, prevents FLiBe leakage and allows the FLiBe operating temperature window.
- A metallic jail that prevents contact among pebbles and ensure the structural integrity of the packed bed.

Another key aspect of liquid breeders is the MHD and magnetic loading on metallic structures, which may causes high pressure drops, low heat transfer coefficients and structural integrity issues. In the present design MHD load are restricted to the encapsulated FLiBe, where MHD effects are low (see e.g. [14]) and where the metallic shell and pipe layout can be designed to minimize any effect. Note that if a ceramic non-conducting material is used, the MHD are dramatically minimized.

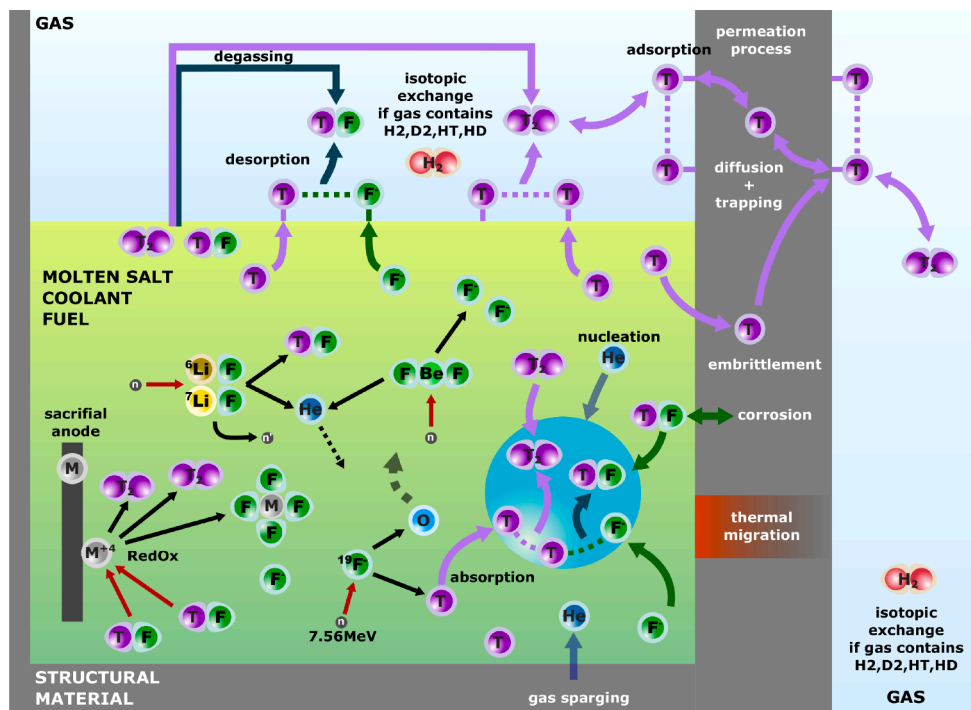


Fig. 1. Summary of T transport in FLiBe.

3.2. Cooling system

Many coolant options exist for BB. Either the breeder material is the coolant (dual concept) or a liquid (e.g. water) or a gas (e.g. He) is used. The use of a liquid coolant was discarded to prevent in-box LOCA events as well as due to chemical compatibility and T extraction. Among the cooling gasses, He is probably the best one as it is transparent to radiation and has very good heat transfer capabilities. However, as the study focuses on a commercially viable solution, He is not the preferred option as it is a very scarce gas with a high market price. In addition, He requires a large pumping power and operating pressures above 7MPa. Therefore, a compromise between activation and heat transfer capabilities was sought.

Nitrogen (N^{16}) is known to have a significant interaction with thermal neutrons (see [18]) and is even used as a shut-down gas for gas cooled reactors. However, it is a very cheap gas that requires lower pumping requirements than He and works with conventional power generation technologies. Some reactor concepts using N_2 or even air as coolant in a direct power generation cycle exist (see [19] among others).

3.3. Multiplier

On one hand, there exist many concepts where either Be or a Be compound is used. Be has a high multiplication factor, but it generates T through the generated Li by the $Be^9(n,2n)Li^7+H^3$ nuclear reaction for $>10.5MeV$. Pure metallic Be and Be compounds like $Be_{12}Ti$ have the same issues as the breeding ones as a sweep gas is needed to remove T, the accumulated T inventory reduced the operating time of the blanket and swelling is also expected to be a major issue [20].

On the other hand, Pb is also used as a multiplier as $Pb^{208}(n,2n)Pb^{207m}$ for $>7.4MeV$. One advantage of using Pb is that no carrier gas is needed as no T is generated. However, more multiplier is needed to achieve the same multiplication factor as that of Be and the low melting temperature of pure Pb (327.5°C) may be a problem. Several lead compounds, e.g. the inter-metallic Zr_5Pb_4 have been proposed, but they are scarce or difficult to synthesize with the available technology as far as the authors know.

The present design proposes the use of a Pb compound to prevent the use of Be, which is scarce, toxic and generates T. A good candidate would be Zr_5Pb_4 , but a compound with a lower content of lead (see [12]) like PbS might be a better option as it is abundant and has a low price when compared to all the aforementioned multipliers. PbS has also a high melting point so it can be placed between the coolant pipes as a pebble bed. Furthermore, Zr_5Pb_4 is known to contain hafnium impurities that are difficult to remove due to a similar chemistry to that of zirconium. Hafnium is a very effective neutron poison for fast neutrons, so it will negatively impact the TBR. Using PbS will result in a Be free blanket with a lower TBR. However, this can be compensated by optimizing the configuration.

In the present study PbS is not used as the blanket multiplier in the calculations because a complete study, out of the scope of the present paper, must be carried out for this compound to be considered.

3.4. Reflector and shielding

The use of a reflector to improve the neutron economy of the blanket and generate more T is also a good option to reduce the total thickness of the blanket. Low Z reflectors like boron or graphite are known to be efficient reflectors for thermal reactors. However, the neutron energies of a fusion reactor are too high for these reflectors to work properly. High Z reflectors work better for fast neutrons, but they might not be efficient for scattered neutrons generated by the multiplier and the breeder. As a result, compound like tungsten carbide (WC) or tungsten boride (WB), which have good mechanical properties and vacuum compatibility, can be used to cover the range of neutron energies for both shield the back of

the blanket and increase the TBR. Note also that these materials have good thermo-mechanical properties [21] and are very common for tooling, so their availability and cost is not an issue.

3.5. Layout

The blanket design can be summarized as shown in Table 1.

A pebble design example is shown in Fig. 2. Further optimization of the design will lead to optimum thickness for the pebble to degas T and He as well as to operate in the desired temperature window without leaking FLiBe.

The pebbles with a diameter 1–3 cm are slightly loose packed ($\epsilon=0.45$) into the pipes to allow expansion as shown in Fig. 3. Note that the jail, together with the loose packing will allow a better cooling of the system.

The First Wall (FW) structure is detached from the BB. Top and bottom manifolds (see Fig. 4) distribute the flow. The distribution pattern can be optimized to enhance heat transfer, keep the blanket within the working temperatures and for the baking process before operation.

3.6. Structure

3.6.1. Structural material

The maximum thermal efficiency of the blanket is determined by the maximum operational temperature of the structural materials. The selection of the structural material for pipes, manifolds and supports is mainly driven by its activation and its performance at high temperature.

For the materials of interest, most benefit is obtained if we work in the creep regime, avoiding cyclic thermal stress. Indeed, undesirable cyclic loads are penalising the creep regime through the well-known creep-fatigue interaction and progressive deformation.

If the material temperature is reduced (i.e. cold supports, reduced thermal performance), then embrittlement irradiation effects under instantaneous loads (IPFL failure) becomes dominant.

Several materials RAFMs (Reduced Activation Ferritic Martensitic steels) were considered: Eurofer 97, MHT-9, ODS, F82H and ORNL 9Cr-2WVTa. Regarding activation, the lower the Mo, Nb, Ni and Cu content the better. It can be concluded, then, that Eurofer 97, F82H and ORNL 9Cr-2WVTa are the best candidates. When cost and availability for STEP are accounted for, Eurofer 97 seems to be the best option as its mechanical properties allow a temperature window from 300°C to 550°C; for the present work Eurofer 97 was selected.

The material allowables in this analysis for Eurofer 97 were extracted from [22], although HT rules (creep) and LT rules under irradiation (IPFL) are still under discussion [23] [24] [25].

3.6.2. BB Structural concept and applicable loads

The pebbles are designed to leak gases generated inside, while retaining the fluid. As a result, no significant internal pressure is built. Additionally, the jail supports the self-weight and inertial loads of the system, leaving very low structural requirements for the pebble shells.

The jails shall withstand a high temperature with possible thermal cycles in the pebble bed causing progressive deformation and fatigue, being the main concern the effect of fatigue cycles in the creep

Table 1
Materials and configuration of the encapsulated breeder blanket.

Function	Material	Configuration
Structure	Eurofer 97	Electron Beam Welding (EBW)/ milling
Cooling	N_2	Top and bottom manifold with vertical pipes in between
Breeder	FLiBe	Encapsulated in a porous ceramic shell protected by a metallic jail
Multiplier	PbS	Packed bed among pipes

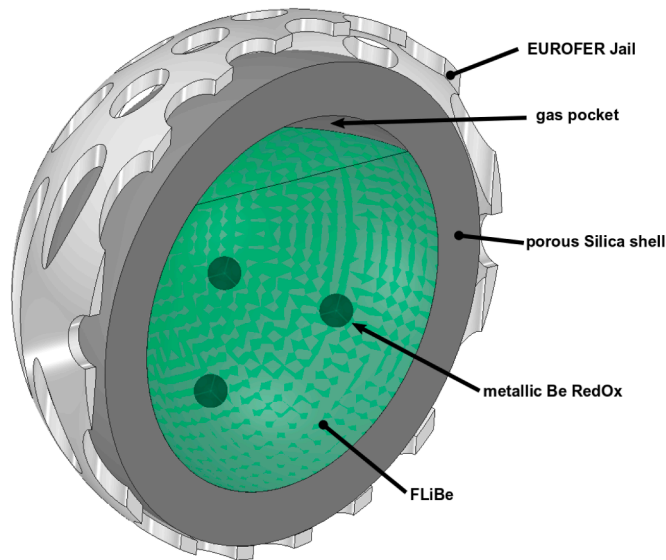


Fig. 2. Example of a pebble design for the encapsulated breeder concept. Sizes are not to scale to show the different components.

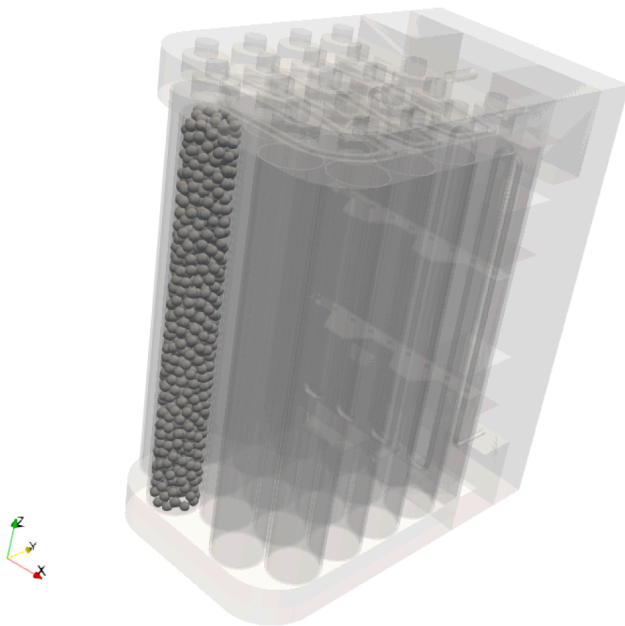


Fig. 3. Packed bed inside one of the cooling pipes.

resistance. Note that the creep-fatigue interaction lowers significantly the allowable membrane stress under constant loads (gravity). Therefore, the pebble bed shall be loose enough to accommodate changes in pebble geometry (no "local" thermal overconstraint) the following provisions shall be ensured:

- Provision to nominal dimensions and tolerances: the pebble bed diameter tolerances and the pipe inner diameter cannot be packed in a horizontal plane, avoiding 2D-like locking in the pipe section.
- Provision to volumetric expansion: the pebble bed expands in the axial direction of the pipe. Then, the distance to the pipe end shall be sufficient to accommodate a pessimistic expansion case, at least in most of the working cycles producing fatigue

Note that EM loads and thermal loads are opposite design drivers: EM loads require stiff structures, while thermal loads work better with

unconstrained structures. The pipe-manifold structural topology releases some structural constraints to enhance thermal behaviour, but EM behaviour can be compromised. To this aim, the structural topologies in Table 2 were assessed. Note that free supports do not exist in practice, since they are not able to withstand any EM load. However, the concept is very useful for the thermal design.

Some concepts, e.g. the HCPB, use a box structure, which is very stiff, while the pipe-manifold is more compliant. An intermediate solution is a honeycomb structural concept. Also, hybrid structures between mixing pipe-manifold and honeycomb-like may arise in further optimization exercises.

An important aspect of the presented design is the low mass of structural material since efficient structures (pipes vs plates) have been used.

4. Blanket analysis

A series of analyses have been carried out to assess the feasibility of the design towards a conceptual design. Note that further analyses, which are out of the scope of the present study, are needed to achieve a robust conceptual design.

4.1. Neutronics

A parametric neutronic analysis for the proposed blanket was performed. More than 120 cases were run with an error below 5%. The CAD geometry was translated into an OpenMC© parametric geometrical model as shown in Fig. 5 where components thickness and material distributions could be changed. The pebble packed bed was generated with the OpenMC© packing generator and the TRISO model. The TBR of a blanket depends on the geometrical parameters of components of the blanket as well as on the materials of these components. Therefore, a multi-parameter optimization problem must be solved for a TBR > 1. In order to reduce the amount of analyses, the problem has been split in two: the geometrical optimization and the material optimization. This methodology assumes that the effect of the materials on the sensitivity analysis of a given geometrical parameter does not change from the tendency standpoint. This fact is also checked during the analysis of the sensitivity to the materials results.

4.1.1. TBR Sensitivity to components thickness

A sensitivity analysis to the parameters shown in Table 3 was performed assuming Be₁₂Ti as multiplier, WC as reflector, Eurofer 97 as structural and jail material, Silica for pebble shell and metallic Be as the redox controller of the breeder material, which is FLiBe (enriched to 95% Li⁶). The coolant was selected to be N₂ and the blanket space among pipes was left to be vacuum. The packing void fraction of the pebbles was kept low at 0.45 to save computational time. As a result, low TBR were expected, but the difference between geometrical parameters was significantly augmented.

Results (see Fig. 6) show that as the First Wall thickness is increased, the TBR decreases, which is expected as the First Wall shields neutrons that are either reflected, absorbed or moderated. Either way, the amount of neutrons with energies above 14MeV reaching the breeder region becomes less. The same happens with the thickness of the multiplier region before the breeder region. As the multiplier thickness increases, the TBR becomes lower.

The impact of the manifolds thickness is slightly different. The thicker the manifolds, the less breeder there is. Hence, it is expected that the TBR becomes lower as the thickness increases. However, the structural material in the manifolds works as a multiplier to some degree. This means that for thin manifolds, as the thickness increases, the TBR is also higher. This happens until the multiplication effect is no longer compensating the reduction in the breeder material region.

It can be seen that thinner First Wall and manifolds combined with a

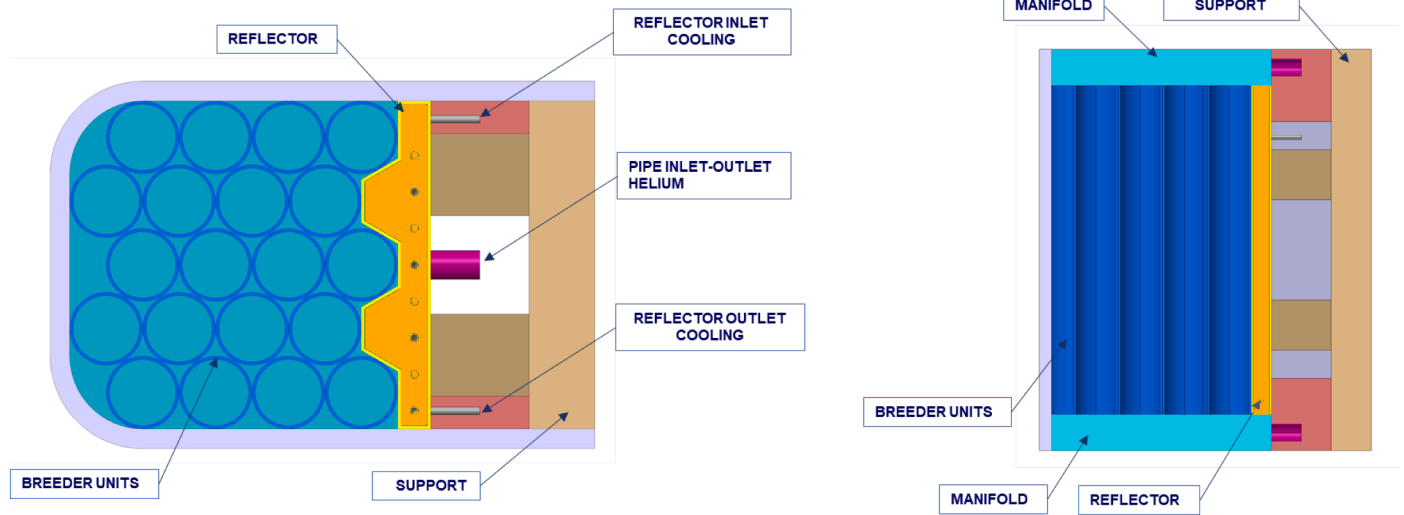


Fig. 4. Preliminary blanket design with the vertical pipes in-between manifolds. Note that blue color on the left picture belongs to the manifold as the tubes do not contain neither the pebbles nor the multiplier for simplicity. (For interpretation of the references to colour in this figure legend, the reader is referred to the web version of this article.)

Table 2
Structural topologies for analysis.

Config.	Blanket	Supports
PU	Pipes with manifolds	Free
PC	Pipes with manifolds	Fixed
HU	Honeycomb	Free
HC	Honeycomb	Fixed

Table 3
Matrix for the sensitivity analysis to component thicknesses. The combination of these values conforms the set of cases run.

Parameter	swept values
First Wall(cm)	2, 4, 6
Multiplier(cm)	1, 5, 10
Manifold(cm)	3, 6, 9
Breeder diameter(cm)	1.85
Shell thickness(cm)	0.15
External jail diameter(cm)	2.02
Jail thickness(cm)	0.15
Reflector(cm)	5, 15, 20

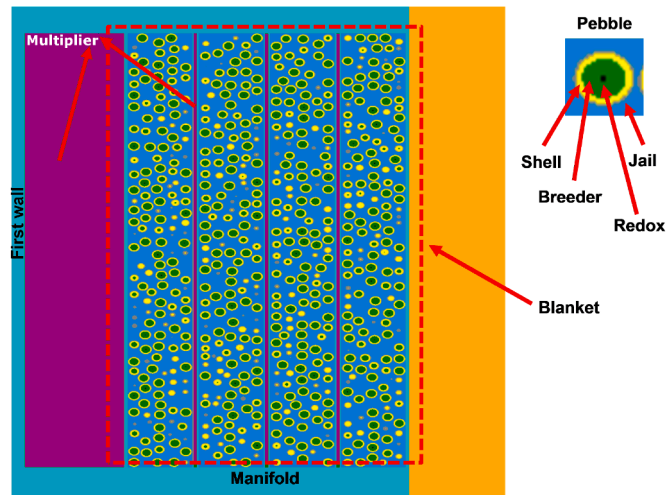


Fig. 5. OpenMC parametric simplified 3D geometry slice for the blanket analysis showing the pebbles in each pipe. The slice presented is through the center of the blanket, so multiplier among pipes is very thin. In addition, the presented model shows a thick multiplier region at the front, but different thicknesses were calculated.

multiplier placed among the breeder is the most promising configuration.

The impact of the reflector on the TBR is almost negligible. The energy of the neutron that are reflected back into the breeder zone is too low to breed T any more. It can be concluded that the reflector should be included elsewhere if the neutron economy is to be improved. One possibility is add the reflector before or around the manifold.

4.1.2. TBR Sensitivity to component materials

A TBR and a Helium Breeding Ratio (HeBR) sensitivity to different materials were performed assuming a single design point: 2cm First Wall, 6cm for the manifolds, 10cm for the reflector. A sensitivity to the multiplier thickness was carried out to check the material independence with respect the previous sensitivity analysis. In this analysis the space among pipes was filled with the multiplier.

The highest TBR cases were selected (see Fig. 7) as potential cases for optimization. Both Be and Pb based multipliers achieve TBR>1, but, only Pb based multipliers at the front improved the TBR significantly. Beryllium is a scarce material that has been the object of several studies to reduce its content in blanket designs (see, e.g., [26]). In addition, its handling is very dangerous because of its toxicity, so a Pb based blanket seems a better option than a Be one. Regarding the reflector, both WC and SiC gave similar TBRs. The HeBR is lower for SiC than for WC, which is an advantage.

4.1.3. Detailed analysis of the base line case

A detailed analysis of the Zr₅Pb₄based blanket configuration with SiC as the reflector, which led to a TBR~1.1, was selected as a base line case in order to detect key local features.

The neutron flux at different neutron energies is shown in Fig. 8. The expected exponential decay is observed across the blanket, dropping two orders of magnitude at the back of the reflector region. It must be noted that most of the flux is located between the First Wall and the second row of pipes. In addition, a small plateau can be observed in the 1 to 5MeV energy bin at the front of the blanket, which correspond to the multiplier region. This suggests that the blanket can be further optimized by

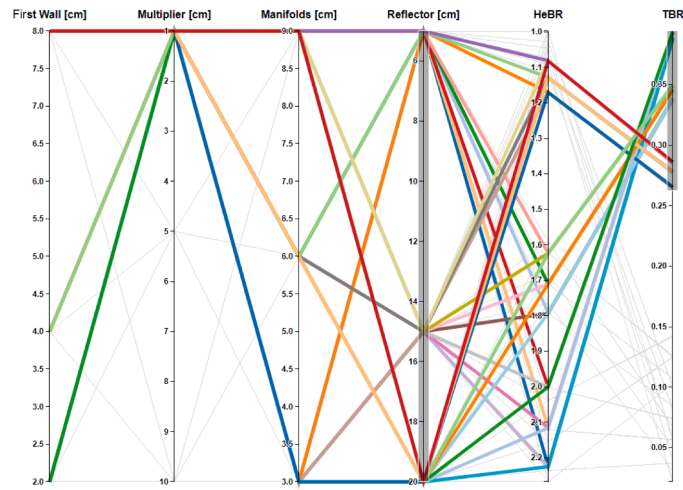


Fig. 6. Analysis of the TBR sensitivity to different component thicknesses. The highest TBR have been highlighted.

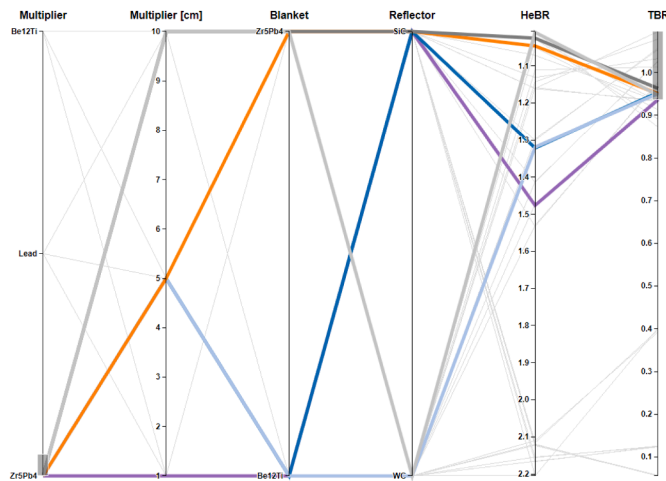


Fig. 7. Analysis of the TBR sensitivity to different materials at different functional regions of the blanket. The highest TBRs have been highlighted.

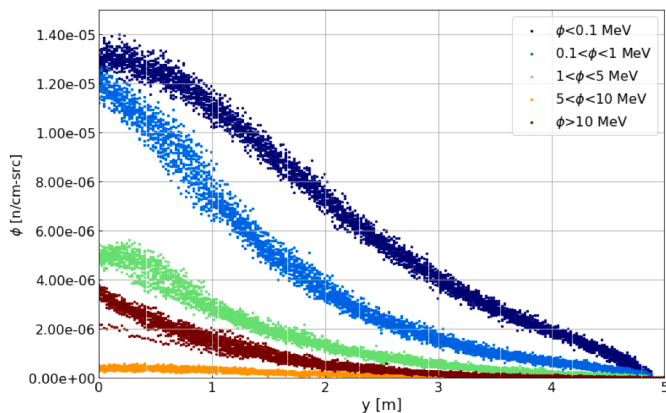


Fig. 8. Neutron flux profile for an equatorial slice. Scattering corresponds to different values at different cells across the slice.

allowing more multiplier among the pipes and less thickness at the front region.

Despite that the First Wall configuration was left out of the scope of this study, it is clear that its design has a huge impact on the TBR. This

can be observed by the low neutron energy flux at the front of the blanket. The more transparent to the neutrons the First Wall is, the higher the TBR. However, this is technically very difficult as, among other things, it must withstand high heat fluxes ($>1\text{MW}/\text{m}^2$).

The resulting nuclear heat deposition is shown in Fig. 9 for a First Wall neutron flux of $2 \cdot 10^{14} \text{ n}\cdot\text{cm}^{-2}\cdot\text{s}^{-1}$. Note that neutron rates in a compact spherical tokamak can reach up to $1 \cdot 10^{19} \text{ n}\cdot\text{s}^{-1}$ (see [27] among others). The peak H reaches a value of $14.8\text{MW}/\text{cm}^3$ at the breeder material. The structural material at the front of the blanket (First Wall and manifolds) reaches power depositions around $1\text{MW}/\text{cm}^3$. Therefore, the blanket cooling scheme must focus on the packed bed cooling and on the front structural material. It can be concluded as well that the back reflector in the present configuration may not need active cooling as it has a low deposition around $0.001\text{MW}/\text{cm}^3$.

The T generation only occur inside the pebbles (see Fig. 11) as no Be based multiplier was used in this configuration. The TBR follows the neutron flux tendency as expected and shown in Fig. 10. However, as the each pebble in the packed bed was modelled, data is scattered. Note that the pebbles in the cooling pipes at the back of the blanket have a very

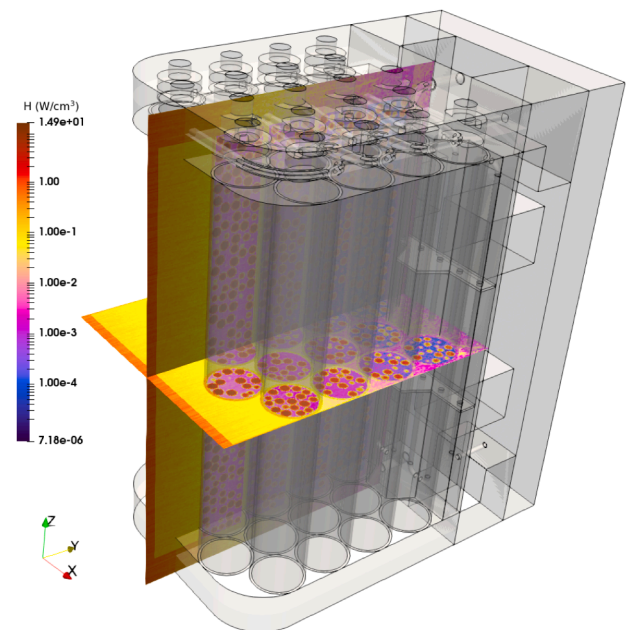


Fig. 9. Nuclear heat deposition distribution on two slices through the center of the blanket. Maximum deposition is located inside the pebbles.

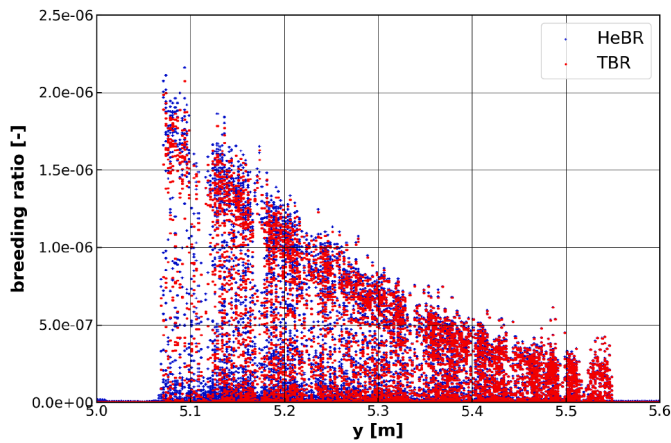


Fig. 10. TBR and HeBr profile for an equatorial slice. Data is scattered due to the discrete modelization of all the pebbles in each pipe.

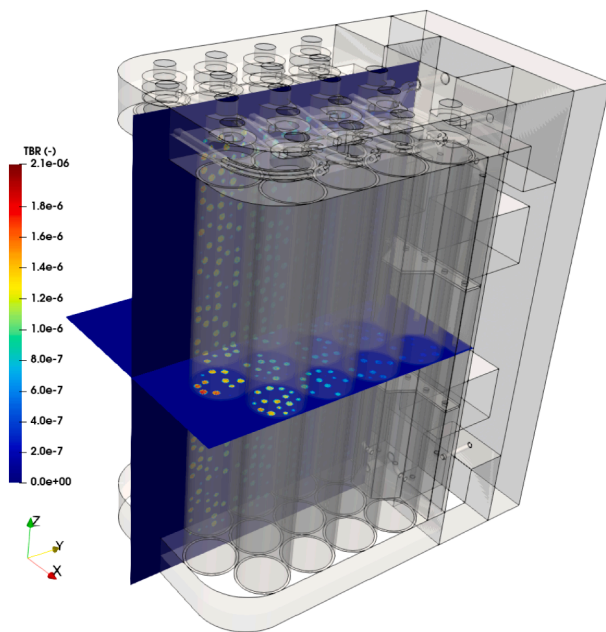


Fig. 11. TBR distribution on two slices through the center of the blanket. T is only generated inside the pebbles.

small TBR, but still significant. Note also that most of the neutrons are absorbed by the FLiBe in the pebbles before the back of the blanket.

The coolant through the packed bed should extract all the T generated in the blanket, so no carrier would be needed for the multiplier or elsewhere.

The HeBR is slightly higher than the TBR as He is also generated in the structural material and the multiplier. It can be observed as well that the HeBR is slightly higher in the first wall than in the multiplier but no significant swelling is expected as it would in Be based multipliers.

It can be concluded that the current pre-conceptual design is feasible from the neutronics point of view and allows further improvement to achieve higher TBR as well as to minimize neutron leakage.

4.2. Thermal-hydraulics and t transport

For a preliminary thermal-hydraulic analysis, two simplified models were generated, a single pebble that included the shell, the breeder and gas pocket, and a full pipe model including the packed bed with the exact pebble distribution as that in the neutronic calculations. Both

simulations are used as representative cases for the feasibility analysis of the blanket.

4.2.1. Pebble model

A single pebble model was generated to assess the internal thermal hydraulics and T transport in the FLiBe and the gas pocket. The model was run as an unsteady case with the Volume of Fluid (VOF) method using the CFD software STARCCM+® until a steady state was reached. Momentum, energy and T concentration as a passive scalar were modelled. The heat source and T generation terms were extracted from the neutronic baseline case results corresponding to a pebble in a front pipe (the closest pipe to the first wall). The FLiBe properties were chosen to be temperature dependent from [28] and the gas in the pocket was modelled as an ideal gas. The external surface of the shell was set to a constant temperature of 900°C. All the regions were solved coupled.

Fig. 12 shows the results at steady state. The left picture shows the FLiBe volume fraction with transparency (purple to green divergent colour map) and it also includes velocity streamlines coloured by the velocity magnitude (rainbow map). The streamlines show a toroidal vortical structure inside the FLiBe (green volume). This vortex is a convective cell that shows up to enhance heat and mass transport (T) through the shell. The interface stays stable with very little change over time as the relative pressure slightly changes and FLiBe vortex is not strong enough.

The temperature distribution in shown in the central picture of Fig. 12 (blue to red). It shows how the gas pocket has a significant gradient (top region) as well as the highest temperature. The shell stays almost at the coolant temperature (blue color which corresponds to the lowest temperature). The temperature distribution in the FLiBe (pebble center below the gas pocket) has a smoother temperature gradient when compared to the gas as mixing due to the vortex tend to homogenize the temperature.

The T concentration in FLiBe is almost constant due to the vortex. Figure is omitted as very little differences are noticed. T distribution in the permeating shell are shown in the right picture in Fig. 12 (rainbow map). A quarter of the shell is shown for simplicity as results are symmetrical. Most of the T is transported to the gas pocket and accumulates at the top of the pebble as can be observed by the highest values on the top internal region of the shell.

Results show the importance of the gas pocket inside the pebble. Most of the T ends up accumulating in this region, so in order to reduce the T inventory in the pebble (and in the blanket) permeation or T extraction must be enhanced especially in this region. Therefore, the pebble shell must be permeable to T and has to prevent any molten salt leakage during operation.

The material to be used as a membrane permeable to T and He must have a porosity that does not allow FLiBe to leak. To conservatively evaluate this porosity a cylindrical pore across the shell is assumed to evaluate the phenomenon. Note that in case of a pore network, it will improve tightness. The maximum pore size was calculated using Eq. 1 from [29] at different pressure gradients as shown in Fig. 13.

$$r_{max.pore} = \frac{-2B\sigma_{FLiBe} \cos(\phi)}{\Delta P} \quad (1)$$

where r is the maximum radius of the pore that prevents leakage, B is the pore shape coefficient (B=1 for cylindrical pores), σ is the surface tension, ϕ is the contact angle. Parameters were taken from [28].

Results show that pores can be large (>1 μ m) under blanket conditions. This porosity is feasible as exposed for example in [30] among others.

4.2.2. Packed bed model

The pebble packed bed can be generated using three methods. The first method consists of running a soft body simulation with STARCCM+®. The resulting packed bed is very realistic, but lacks the

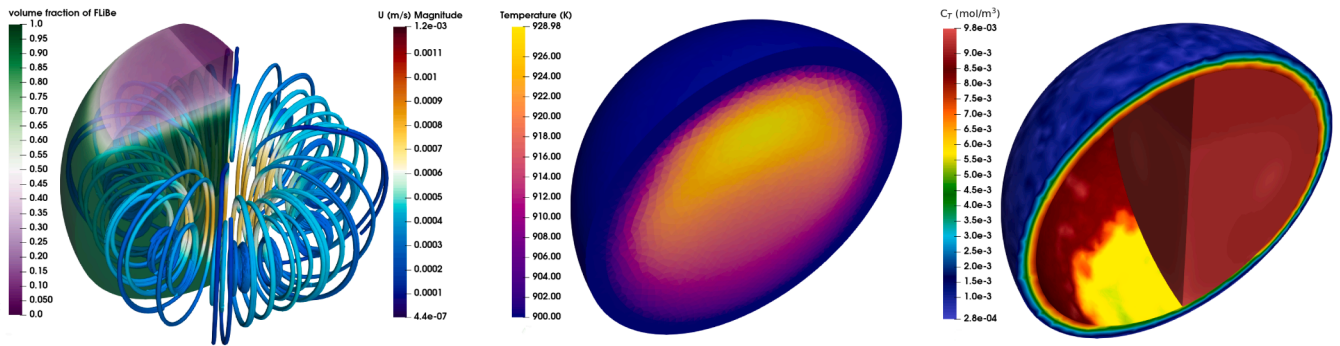


Fig. 12. Single pebble CFD model results at steady state with FLiBe volume fraction (e) (purple to green divergent colour map) and velocity streamlines coloured by the velocity field (U) (blue to red divergent map) in the pebble showing the internal convection cell on the left, temperature distribution (blue to red) and shell T concentration (rainbow map) on the right. (For interpretation of the references to colour in this figure legend, the reader is referred to the web version of this article.)

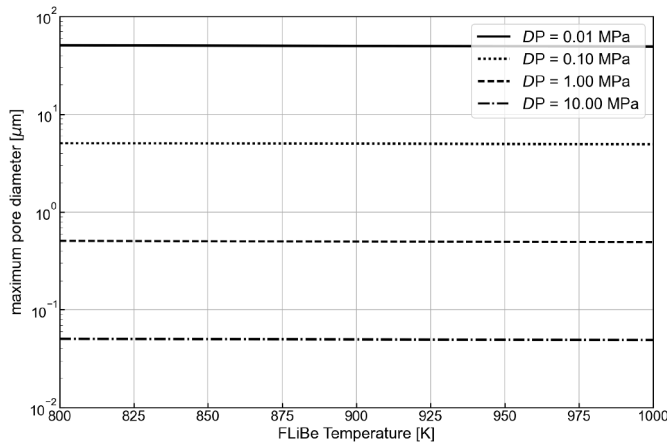


Fig. 13. Maximum pore for shell tightness to molten FLiBe.

conformality with respect the neutronic simulations and is computationally intensive. The second method involves a rigid body simulation (see Fig. 14), which is computationally less demanding (see [31] and references therein), but has the same conformality problem as the spheres will not match the location of the neutronic simulation pebbles. A third method has been implemented, which is to use the coordinates of the center of the pebbles in the neutronic simulation and translate the geometry with a custom script into STARCCM+. Note that the previous methods can be used in advance of the neutronic analysis and the geometry be translated to OpenMC.

A simple thermal hydraulic case using N₂ as cooling gas of a front

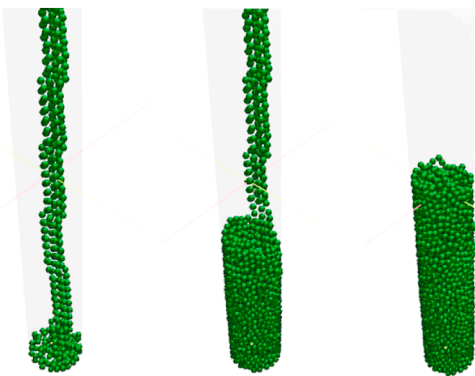


Fig. 14. Discrete element simulation showing a sequence of how a blanket pebble bed is being filled. Resulting pebble center coordinates are used for CFD analysis of the pebble bed.

pipe with an imposed heat flux at the pipe walls and pebbles was setup. The coolant was modelled as an ideal gas at an operating pressure of 1 MPa. A constant inlet velocity of $U_z = -10$ m/s (≈ 8 kg/s) at 573.15 K was set as boundary conditions.

The heat flux has been extracted as an average value from the neutronic calculations for simplicity. In addition, The inlet and outlet boundary conditions was extruded to prevent any boundary related numerical instability. Turbulence was accounted for with the $k-\epsilon$ model with corrections for the curvature of the existing surfaces. The generated polyhedral mesh (see Fig. 15) has >100 million cells and a $y^+ \sim 1$ to ensure a reliable heat transfer. In addition, a prismatic layer has been included to properly resolve the boundary layer.

N₂ flows through the core of the packed bed at a lower velocity than that of the region between the pebbles and the pipe walls. This effect was expected as preferential channels do exist in this kind of configurations, especially close to the walls. A closer look at the flow in the packed bed shows a complex flow pattern at the center of the bed. However, the flow distribution is very homogeneous. The two expected stagnation points at the flow impingement region at the bottom of the pebble and at the other side of the pebble can be observed in Fig. 16.

Regarding heat transfer, the pipe temperature distribution is shown in Fig. 17. The temperature rises towards the outlet leaving some preferential channels along the pipe with a lower temperature. It can be observed that where the pebbles contact the pipe walls hot spots are identified. A similar pattern can be observed for the pebbles surface temperature distribution. A detailed view of the pebbles in Fig. 17 shows how the heat transfer is lower where there are contacts with the pipe wall. The results show a quite homogeneous temperature distribution on the pebbles and an acceptable heat extraction.

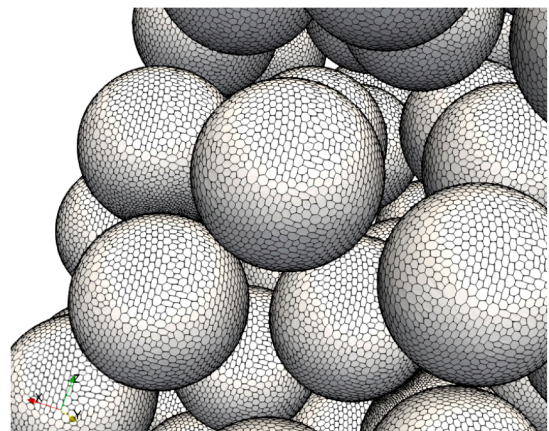


Fig. 15. Detail of the mesh used for the thermal hydraulic analysis of the packed bed.

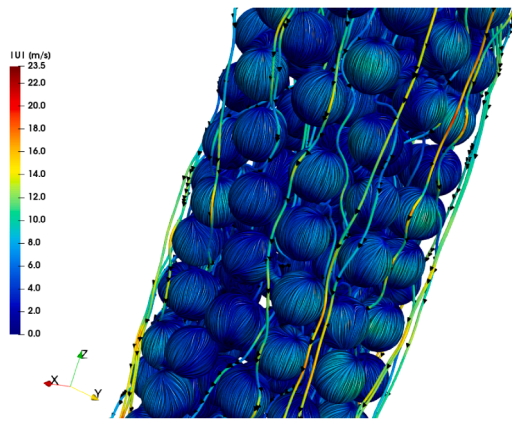


Fig. 16. Packed bed velocity streamlines and Large Integral Convolution (LIC) on the pebbles surface.

This simulation example gives a valuable insight on the thermal hydraulic behaviour of the packed bed and shows that the system can be properly cooled.

4.3. Thermo-mechanical

The thermo-mechanical analysis is presented in three stages: load specification, thermal analysis, and mechanical analysis. The thermo-mechanical simulations were performed with the code Abaqus© 2018 using stationary thermal and mechanical analysis with sequential coupling.

4.3.1. Load specification

Main Blanket loads include thermal loads, internal pressure, inertial loads (gravity and seismic), EM loads. The thermo-mechanical model relies on a high uncertainty on the loads and operational conditions of STEP. In this sense, a dimensioning exercise of pebbles and pipes is done first. Then, a qualitative analysis of the structural concept is presented.

Later, some plausible load scenarios are postulated to see the effects on the material temperatures and stresses on the structural material, and to have an idea of design limits and main design challenges.

Thermal loads are caused by direct plasma radiation and neutronic heat deposition. It is assumed that direct plasma radiation does not affect the BB, as it is stopped by the FW. Thermal loads are applied in a thermal model of the Blanket to obtain a temperature field. The neutronic sources are taken from Section 4.1 and 9 and Table 5 (see e.g. [10], [32]).

Such temperatures are applied as thermal expansion loads to the mechanical problem (one-way coupling), and the material allowables decrease with temperature. Thermal expansion is fundamental for the dimensioning of the structural supports, which constraint the expansion generating stress. Thermal loads may cause compressions in the pipes, so thickness (slenderness) or side supports need to be dimensioned accordingly. Finally, the cooling of the BB shall be balanced to avoid thermal gradients causing local stress.

It can be preliminarily considered that all the heat generated inside the pebbles is extracted by the N_2 flow. This holds true if the heat conduction (driven by the solid thermal contacts between jails) is low compared to the forced convection (driven by the coolant velocity and pressure). Then, the effective HTC at the BU (Breeder Unit) wall can be roughly assumed to be the in-bed HTC of a bed without jails(see [33]). Some operational ranges are depicted in Table 6. Note that some heat extraction occurs also at the supports, with an assumed temperature of 100°C.

Internal pressure shall be driving the thickness of the pipes in the

Table 4

Materials and multipliers matrix for the sensitivity analysis.

Parameter	swept values
Frontal multiplier material	Be ₁₂ Ti, Lead, Zr ₅ Pb ₄
Multiplier(cm)	1, 5, 10
Blanket multiplier material	Be ₁₂ Ti, Zr ₅ Pb ₄
Reflector material	SiC, WC

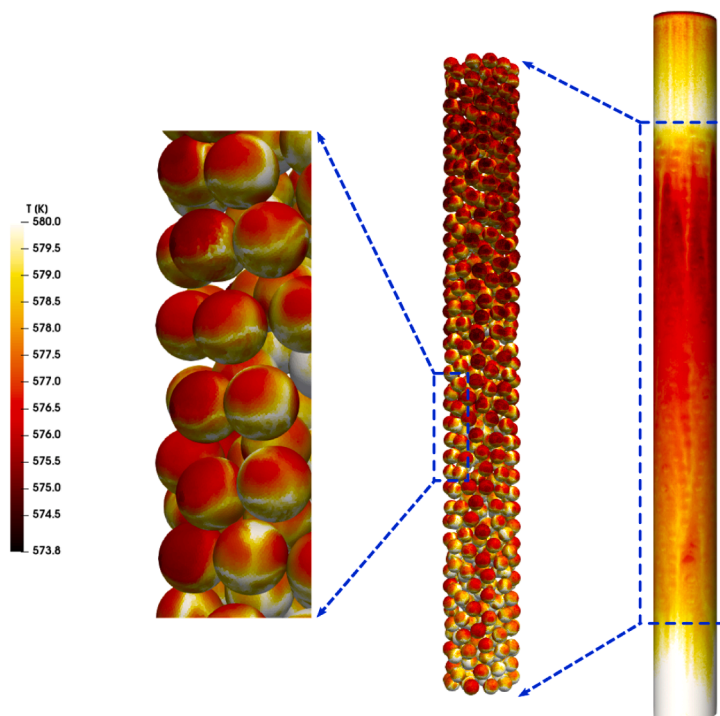


Fig. 17. Temperature distribution in the packed bed.

Table 5
Plasma scenarios.

Plasma	Power (eV/s)	Description
P-1	1.0e18	ITER-like plasma scenario
P-2	1.0e17	STEP-like plasma scenario

Table 6
Cooling scenarios for the BB. Film coefficient was obtained from [33] for pebble heat exchange, pressure drop for 1 BU was calculated from CFD model in Section 4.2.2.

Cooling	Pressure (MPa)	Flow velocity (m/s)	Flow temp. (°C)	Film coefficient ($\frac{W}{m^2C}$)	Δp in 1 BU (Pa)
C-1	1	1	400	432	127
C-2	4	5	400	3708	1232
C-3	8	10	400	10,432	3276

layout (Section 3.6.2). The structural importance of internal pressure determines the applicability of, e.g., PED [34] and ESP/ESPn [35,36], which are very demanding in terms of project supervision, 100% volumetric inspectability of pressure retaining welds, and need of periodic inspections. The NDT (Non-Destructive-Tests) are requested by the C&S (Codes and Standards) after manufacturing. The key joint between pipes and manifolds can be inspected by X-rays, ultrasounds, eddy currents, Q being the final details of the joint determining the preferred technique. Although most C & S use TIG welding as the preferred solution (e.g. orbital welding), other manufacturing techniques (e.g. laser or EBW Electron Beam Welding) are possible with a qualification process and a testing campaign.

Inertial loads (gravity and seismic) are dependent on the seismic behaviour of the placement of STEP while EM loads are generally more demanding.

EM loads arise as Lorentz forces produced by plasma disruptions, and Maxwell forces due to the ferromagnetic nature of the BB structural material. These EM loads are expected to dimension the blanket structures, especially the supports. Additionally, due to the topological features of slender pipe structures discussed in Section 3.6.2, EM forces need to be estimated and checked in the pre-conceptual phase. The EM

loads are dependent on plasma disruptions, which is a characteristic of STEP. Based on previous work in ITER [37], the EM loads are approximated as a linear distribution of volumetric forces in space that creates reactions of about 400 kN in each of the 4 supports considered. Several scenarios are postulated: Moment-Y (torsion), Moment-X (bending), Double-Moment-Z (torsion), ... Moment-X (bending) is identified as the most critical scenario, with very similar results for topologies PC and HC.

4.3.2. Global thermal behaviour

The thermal behaviour of the load ranges in Section 3.6.2 has been studied. The temperature distribution for P-1 and C-2 is shown in Fig. 18. In the proposed geometry, the multiplier experiences significant heating at the front area. However, the temperature is driven by the distance to the cooling (BU pipes), so a different pipe configuration can minimize this issue. Additionally, the highest temperature in the structural material is located at the front (top and bottom manifolds), falling in the High Temperature region of Eurofer 97 (above 450°C). Some front sections of the BU pipes also fall in the High Temperature region, but the problem is closely related to the overheating of the multiplier.

The temperature profiles for different plasma and coolant configurations are analogous, and the quantitative changes in maximum values are reported in Table 7.

4.3.3. Global mechanical behaviour

The pipe thickness can be dimensioned based on internal pressure (primary load). The high temperature pipes are driven by their creep resistance. The pipe dimensioning must take into account that the creep allowable S_t shall be checked instead of the instantaneous allowable S_m

Table 7
Thermal results: maximum temperatures for different plasma and cooling scenarios.

Plasma	Cooling	Multiplier (°C)	Structure (°C)
P-1	C-1	1751	677
P-1	C-2	1588	551
P-1	C-3	1571	534
P-2	C-1	535	427
P-2	C-2	518	415

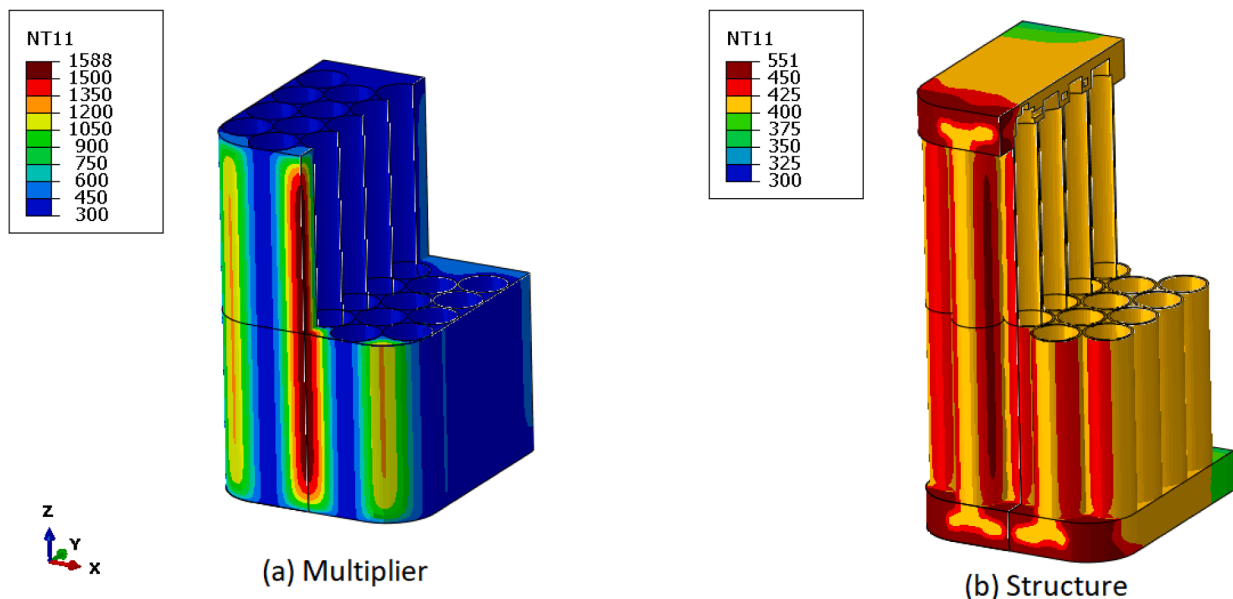


Fig. 18. Temperatures on the multiplier (left) and the structure (right) for plasma P-1 and cooling C-2.

(see RCC-MRx in [38]). Assuming an outer radius of the pipes of 56 mm, the different thickness depending on the temperature, the internal pressure and loads are shown in Table 8. Provisions shall be taken to minimize thermal stress, for instance enabling free thermal expansion in the axial direction of the pipes with an adequate design of the supports. Note that if the fatigue is not reduced by design, a significant drop in the allowable stress is expected.

The mechanical assessment is reported for the thermal loads with plasma P-1 and coolant C-2. The internal pressure has been taken as 8 MPa, which is very convenient for efficiency of the Brayton cycle if a single-loop plant is used [39].

It can be assumed that the creep-fatigue interaction criterion is valid for dimensioning the structure working in the HT range (front pipes, front manifold areas). Provisions against creep damage shall be taken for constant primary loads (gravity + pressure). Since the creep allowable S_t is strongly dependent on the creep-fatigue interactions, provisions against cyclic thermal loads shall be taken in the design, Section 3.6.2.

Additionally, thermal cyclic loads produce progressive deformation (Level A) for cyclic secondary loads (pressure + gravity + thermal), which involves higher loads but also higher allowable $3S_m$. However, for Eurofer 97 in the LT range, these are enveloped by the instantaneous secondary loads, which are limited by the more stringent IPFL (Levels A and C) with allowable S_e . The most demanding behaviour at the cold areas of the BB (support, rear manifold areas, rear pipes) is shown for HC topology with plasma P-1 and cooling C-2, Fig. 19 and Fig. 20.

The thermal cyclic loads for the structure HC loaded with plasma P-1 and cooling C-2 is presented in Fig. 21, together with its potential for mitigation using a structural type PU. Remarkably, the most fatigued zones are not located at the front, mitigating creep-fatigue interactions in the HT areas: the fatigue at the front is driven by local gradients at thermal hotspots. Conversely, the loads at the cold areas and supports are significantly affected by the overall structural temperature, and the stiffness of the connections to the supporting structures. A detailed assessment of the supports needs to be carried out for more advanced design stages.

4.4. Manufacturability

Among liquid breeders, one of the most stable, safest and easy to manufacture is FLiBe. Taking advantage of its low melting temperature, FLiBe can be enclosed even in solid state, while breeding at reactor operation temperatures as a liquid. Available processes are focused on Styropor® coatings (see [40], namely, polymers with very low mechanical properties and melting point 240°C). Current process is readily available to produce hollow spheres with a small access (as a hole in the ceramic shell) where the breeder material (FLiBe) is inserted, then the hollow sphere is sealed. In this case, the mixture breeder-ceramic green material is avoided, but the sealing of the sphere might lead to similar problems. Note that alternative processes based on growing layers of ceramic on "frozen" pebbles of breeder could be extremely beneficial.

As has already discussed the preferred metallurgical alloy is Eurofer 97. The material can be cold worked to obtain seamless pipes in large batches, sheets, and wrought material for the manifolds; no difficulties are expected. The manifolds can be either manufactured by TIG, orbital

Table 8

Selection of thickness for the BU pipes due to inner pressure: sensitivity analysis. The design shall enforce low fatigue usage factor ($1/V$) through free axial thermal expansion or non-cycling loads to reach thickness below 5 mm.

T (°C)	P (MPa)	th _{V=0} (mm)	th _{V=0.2} (mm)
500	4	0.96	4.48
550	4	1.47	6.67
500	8	1.88	8.30
550	8	2.87	11.91

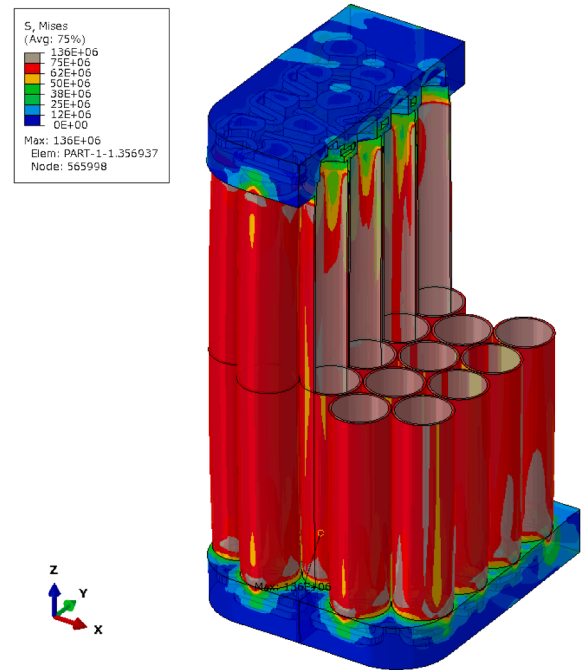


Fig. 19. Mises stress [Pa] for HC structure with monotonic primary loads: plasma P-1, cooling C-2, internal pressure 8 [MPa], gravity, EM Moment-X (bending). This load case dimensions the hot areas of the BB (front manifold areas, front pipes) to be provisioned against creep and creep/fatigue (allowable S_t).

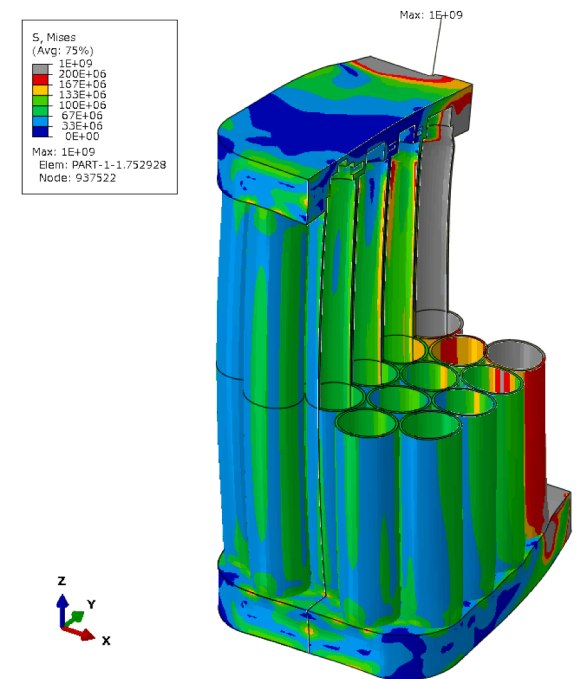


Fig. 20. Mises stress [Pa] for HC structure with monotonic primary and secondary loads: plasma P-1, cooling C-2, internal pressure 8 [MPa], gravity, EM Moment-X (bending). This load case dimensions the cold areas of the BB (support, rear manifold areas, rear pipes) to be provisioned against IPFL (allowable S_e).

welding and Electron Beam Welding (EBW) (Fig. 22) among others.

An important feature is the assembly of closure lids, enabling the breeder to be introduced at a late stage in the assembly; the heat

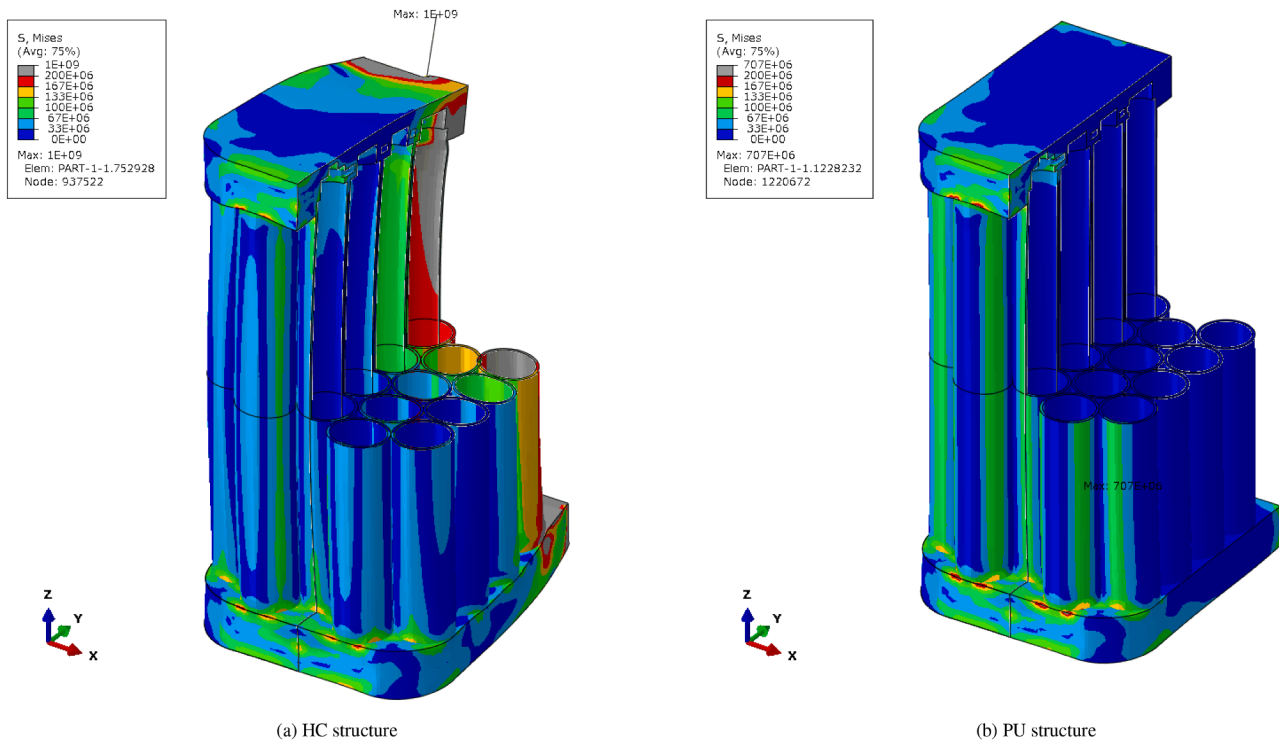


Fig. 21. Mises stress [Pa] for cyclic loads in highly-constrained HC (a) and slightly-constrained PU (b) structures: plasma P-1, cooling C-2.

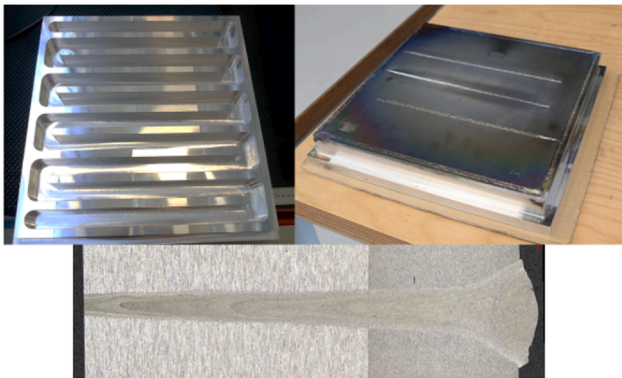


Fig. 22. Nuclear AMRC Aluminium cooling block and E-Beam penetration profile on the same part.

treatment of the final lids can be done locally (without affecting the breeder). The multiplier and the reflector can be placed outside the pipes as packed bed (small pebbles or compressed powder). For structural finishing, a CFC plate can be fitted into the assembly. It is important to mention that the configuration leave very little space (3mm) among pipes, which might make difficult to inspect welds. Leaving the necessary space for inspection will have an impact on the TBR, so must be accounted for in future steps of the design.

4.5. Safety and waste management

The main aspect of a working BB is safety, so the following must be enforced:

- All the blanket materials have to be chosen so that activation is reduced as much as possible.
- Use of non-toxic materials.
- Leakages of activated fluids shall be avoided.

- Prevent or mitigate accidents (e.g. LOCA).
- Easy waste segregation.

The breeding material contains Be, which is encapsulated in the pebbles. Note that the design is breeder-leakage resistant: if the liquid breeder leaks out a pebble, it will either flow to the lower manifold or solidify. To provision the former case, the manifold contains a lower plenum that allows leaked breeder to accumulate without having an impact on the blanket performance. In the later case, the FLiBe will either seal the pebble upon solidification or precipitate to the lower manifold. The low vapour pressure of FLiBe also prevents in-box LOCA.

The main issue working with N is not only its activation (see e.g. [18]), but also the $N^{14}(n,p)C^{14}$ nuclear reaction which has a significant cross-section for fast neutrons [41]. It can be assumed that radiocarbon will have to be removed from the system. Note that radiocarbon is also generated in nuclear water reactors [42] and in graphite reflectors, so the technology for removing it from the coolant streams is well-known.

Regarding the PbS multiplier, the nuclear reactions with sulphur generate radioactive isotopes with half lives below 90 day, like $S^{35}(n,\gamma)S^{34}$ with 87 days. Note that a common problem with Pb is that Po^{209} and Po^{210} and Bi radioactive isotopes are generated. However, using purified Pb for PbS should reduce the problem dramatically as discussed elsewhere [43]. Note also that as PbS does not generate gasses, in-box LOCA is not possible.

The use of WB as reflector may generate T and He [44] due to the $B^{10}(n,\alpha)Li^7$ reaction. However, depending on the design the generation can be dramatically reduced as the neutron absorption probability rapidly decreases below 2.5MeV. If WC is used, He will also be generated along with Be^9 due to the $C^{12}(n,\alpha)Be^9$, but swelling is the only expected issue. Note that dynamic controlled reflectors can also be implemented (see e.g., [45]) to increase or tune the TBR.

The presented design uses a RAFM steel as structural material, which has enhanced radiation activation available material compared to the parent material ASTM P91, and can work with the selected blanket operating temperature window and mechanical loads.

Waste segregation has been accounted for in the design by the assembly sequence: the multiplier and the reflector can be removed by machining the assembly lids, then the pebbles can be extracted from the pipes and can be processed separately. Afterwards, the structural material is isolated from breeder and multiplier. Concerning the pebbles, as FLiBe will be solid once the blanket is removed from the reactor, cutting the jail and crushing the shell for processing should not be an issue.

It must be highlighted that a detailed activation analysis must be carried out to fully assess the impact of using such materials. This analysis is out of the scope of the present study as a more mature design is needed.

5. Conclusions

The presented concept shows the possibility of manufacturing a blanket with conventional techniques at a reduced cost compared to other designs and a $TBR > 1.1$.

The design uses nitrogen to cool the blanket despite other coolants (e.g. He) are known to have a better performance, but they are either scarce or have large pumping requirements. Nitrogen can also be used in a direct power generation cycle and it not only cools down the structure, but it also removes T from the breeder (dual coolant concept). This configuration allows a single pressurized system, reducing the complexity of the blanket. As the coolant also carries T, the N activation, which is less significant, poses no problem for the system. Note that by selecting a gas coolant instead of a liquid metal, water or a molten salt, the corrosion (among other phenomena) is no longer a critical problem.

The cooling scheme is simple from the performance and the manufacturing points of view: a series of vertical (poloidal) tubes, connected by a top and bottom manifold distribute the coolant from front (plasma side) to back. Therefore, the pressure requirements are limited to the pipes and the two manifolds.

The breeder material has been tentatively selected to be FLiBe, which also contributes to the neutron multiplication. The working temperature of the blanket is mainly limited by the material working windows. The structural material, Eurofer 97, works between 300°C and 550°C. FLiBe eutectic 0.531 has a melting point of 363.5°C (with very high viscosity) which increases until 458.9°C for the 0.328 X-eutectic (with lower viscosity), which has a 2:1 LiF:BeF₂ composition. Therefore, the breeder will be liquid in operation, but can be solid during manufacturing. Note that T extraction is improved by having the breeder material in liquid state.

Note that the breeder material generates He at a similar rate as T, then an extraction method that prevents He pressure build up is necessary. The design encapsulates the breeder material in pebbles that allow the extraction of He and T through a porous shell while keeping the breeder contained; two barriers are then present, the pebbles and the pipes.

The pebbles have been designed as a porous shell containing the FLiBe surrounded by a metallic jail. The jail prevents contact between porous media and helps the bed structural integrity. This design also ensures that any FLiBe leakage does not stop the blanket safe operation. Note that the design allows different breeder materials as they are contained in single pebbles.

An additional multiplier is necessary to achieve a $TBR > 1$. In spite of a lower Pb content than other compounds, PbS was proposed because it is available in large quantities at a very low cost. The proposed structural topology enables the use of different multiplier materials filling the space among pipes.

A reflector was also considered at the back of the breeder zone. The neutronic simulations showed that the reflector was not necessary at this location, as it only works as shielding. In further design refinements, it could be used to maximize the neutron flux in the blanket by shielding the manifolds at the front and facing the pipes. The reflector can also be conceived as part of the multiplier packed bed.

The mechanical design is based on a topology of pebbles inside pipes,

with upper and lower manifolds. These pipes are pressurized, and shall also withstand EM and thermal loads mainly. The selection of structural topology aims at alleviating thermal constraints to improve the thermal behaviour.

The thermo-mechanical analysis of these Eurofer 97 structures depends strongly on the blanket temperature (driven by the plasma and cooling operational conditions of the fusion plant), coolant pressure (driven by cooling), and the EM loads (driven by the plasma characteristics). A sweep of operational plasma, cooling, and EM conditions was made, reporting results presumably more conservative than the likely operational cases. The thermal results show a localized heating at the front areas of the BB, with several design corrections to be implemented, and manageable "pessimistic" conditions: ITER plasma, 8 MPa, intermediate HTC. The mechanical results show creep problems at this hot area, but the creep-fatigue is less critical because thermal alternating stresses are expected mainly in the cold areas. Additionally, the loads at the cold areas and supports are significantly affected by the overall structural temperature, and the stiffness of the connections to the supporting structures. The proposed structural concept gives freedom to increase the degree of constraint up to a honeycomb structure to improve the EM behaviour.

The manufacturing of pebbles shall be based on ceramic coatings and hollow spheres (Hollomet). The readily available existing processes do not allow to create tight spheres grown on FLiBe material, then some research (with a sound baseline process) is required.

The manufacturing of the structure is feasible for Eurofer 97, based on state-of-the-art technologies. Such technologies can make use of EBW or orbital welding. No stoppers were found for the current design stage.

CRediT authorship contribution statement

J. Fradera: Conceptualization, Methodology, Investigation, Software, Writing – original draft, Writing – review & editing, Visualization. **S. Sádaba:** Conceptualization, Methodology, Investigation, Software, Writing – original draft, Writing – review & editing, Visualization. **F. Calvo:** Project administration. **S. Ha:** Supervision, Project administration. **S. Merriman:** Supervision, Project administration. **P. Gordillo:** Investigation. **J. Connell:** Investigation. **A. Elfaraskoury:** Project administration. **B. Echeveste:** Resources, Project administration.

Declaration of Competing Interest

The authors declare the following financial interests/personal relationships which may be considered as potential competing interests:

The presented Breeding Blanket Concept has been filed for patent under patent application EP20383029.4. owned by UKAEA with authors S.Ha, J.Fradera, S. Sdaba and F. Calvo.

Acknowledgements

The authors would like to thank UKAEA and Nuclear AMRC for their collaboration and for providing all necessary data to carry out the presented work.

References

- [1] G. Aiello, J. Aubert, L. Forest, J.-C. Jaboulay, A.L. Puma, L. Boccaccini, Design of the helium cooled lithium lead breeding blanket in CEA: from TBM to DEMO, *Nucl. Fusion* 57 (4) (2017) 046022.
- [2] K. Schleisiek, H. U. Borgstedt, F. Dammel, H. Feuerstein, A. Fiege, U. Fischer, H. Gerhardt, H. Glasbrenner, T. Jordan, K. Kleefeldt, W. Kramer, P. Norajitra, G. Reimann, H. Reiser, G. Schmitz, H. Schnauder, R. Stieglitz, Kernforschungszentrum Karlsruhe(November) (1994).
- [3] L. Boccaccini, N. Bekris, Y. Chen, U. Fischer, S. Gordeev, S. Hermsmeyer, E. Hutter, K. Kleefeldt, S. Malang, K. Schleisiek, I. Schmuck, H. Schnauder, H. Tsige-Tamirat, Design description and performance analyses of the european hcpb test blanket system in iter feat, *Fusion Eng. Des.* 61–62 (2002) 339–344.
- [4] C. Forsberg, G.T. Zheng, R.G. Ballinger, S.T. Lam, Fusion blankets and fluoride-salt-cooled high-temperature reactors with flibe salt coolant: common challenges,

- tritium control, and opportunities for synergistic development strategies between fission, fusion, and solar salt technologies, *Nucl. Technol.* 206 (11) (2020) 1778–1801, <https://doi.org/10.1080/00295450.2019.1691400>.
- [5] R.L. Frano, M. Puccini, E. Stefanelli, D. Del Serra, S. Malquori, Manufacturing technology of ceramic pebbles for breeding blanket, *Materials (Basel)* 11 (5) (2018) 1–9, <https://doi.org/10.3390/ma11050718>.
- [6] R.A. Causey, R.A. Karnesky, C. San Marchi, Tritium barriers and tritium diffusion in fusion reactors, *Comprehensive Nuclear Materials* 4 (2012) 511–549.
- [7] J. Fradera, S. Cuesta-López, The effect of a micro bubble dispersed gas phase on hydrogen isotope transport in liquid metals under nuclear irradiation, *Fusion Eng. Des.* 88 (12) (2013).
- [8] J. Fradera, S. Cuesta-López, Nucleation, growth and transport modelling of helium bubbles under nuclear irradiation in lead-lithium with the self-consistent nucleation theory and surface tension corrections, *Fusion Eng. Des.* 88 (12) (2013).
- [9] J. Fradera, S. Cuesta-López, Impact of nuclear irradiation on helium bubble nucleation at interfaces in liquid metals coupled to permeation through stainless steels, *Fusion Eng. Des.* 89 (1) (2014).
- [10] R.W. Moir, A review of inertial confinement fusion (icf), icf reactors, and the hylife-ii concept using liquid flibe (1989). [10.2172/5343327](https://doi.org/10.2172/5343327).
- [11] M.Z. Youssef, M.E. Sawan, Activation analysis for two molten salt dual-coolant blanket concepts for the u.s. demo reactor, *Fusion Sci. Technol.* 47 (3) (2005) 518–523, <https://doi.org/10.13182/FST05-A736>.
- [12] F. Hernández, P. Pereslavtsev, First principles review of options for tritium breeder and neutron multiplier materials for breeding blankets in fusion reactors, *Fusion Eng. Des.* 137 (2018) 243–256.
- [13] R. Romatoski, L. Hu, Fluoride salt coolant properties for nuclear reactor applications: a review, *Ann Nucl Energy* 109 (2017) 635–647.
- [14] B. Sorbom, J. Ball, T. Palmer, F. Mangiarotti, J. Sierchio, P. Bonoli, C. Kasten, D. Sutherland, H. Barnard, C. Haakonsen, J. Goh, C. Sung, D. Whyte, ARC: A compact, high-field, fusion nuclear science facility and demonstration power plant with demountable magnets, *Fusion Eng. Des.* 100 (2015) 378–405.
- [15] C. Wong, S. Malang, M.E. Sawan, I. Sviatoslavsky, E. Mogahed, S. Smolentsev, S. Majumdar, B. Merrill, R. Mattas, M. Friend, J. Bolin, S. Sharafat, Molten salt self-cooled solid first wall and blanket design based on advanced ferritic steel, *Fusion Engineering and Design - FUSION ENG DES* 72 (2004) 245–275.
- [16] E. Morse, *Fusion Technology*, Springer International Publishing, 2018, pp. 413–479.
- [17] P. Masset, R.A. Guidotti, Thermal activated (thermal) battery technology: part II. molten salt electrolytes, *J Power Sources* 164 (1) (2007) 397–414, <https://doi.org/10.1016/J.JPOWSOUR.2006.10.080>.
- [18] E. Ibe, H. Karasawa, M. Nagase, M. Endo, S. Uchida, M. Utamura, Chemistry of radioactive nitrogen in BWR primary system, *J Nucl Sci Technol* 26 (9) (1989) 844–851.
- [19] J.H. Owston, Reactivity analysis of a direct nuclear heated gas turbine with nitrogen coolants, *Nucl. Eng. Des.* 355 (May) (2019) 110355.
- [20] E. Rabaglino, Helium and tritium in neutron-irradiated beryllium, *Forschungszentrum Karlsruhe* (2004).
- [21] S.A. Humphry-Baker, G.D. Smith, Shielding materials in the compact spherical tokamak, *Philosophical Transactions of the Royal Society A: Mathematical, Physical and Engineering Sciences* 377 (2141) (2019).
- [22] RCC-MRx, Demande de modification / modification request DMRx number: 10–115 A3. gen et A3.19as eurofer dated: 28.06.2010.
- [23] J. Aktaa, M. Walter, G. Angella, E. Perelli Cippo, Creep-fatigue design rules for cyclic softening steels, *Int J Fatigue* 118 (2019) 98–103, <https://doi.org/10.1016/j.ijfatigue.2018.08.008>.
- [24] K. Zhang, J. Aktaa, Ratcheting and fatigue behavior of eurofer97 at high temperature, part 2: modeling, *Fusion Eng. Des.* 152 (2020) 111426, <https://doi.org/10.1016/j.fusengdes.2019.111426>.
- [25] J. Aktaa, Y. Carin, J. Vallory, Non-linear assessment of critical failure modes in the first wall of the european tbm, *Fusion Eng. Des.* 128 (2018) 223–230, <https://doi.org/10.1016/j.fusengdes.2017.11.032>.
- [26] J. Shimwell, S. Lilley, L. Morgan, L. Packer, M. Kovari, S. Zheng, J. McMillan, Reducing beryllium content in mixed bed solid-type breeder blankets, *Fusion Eng. Des.* 109–111 (2016) 1564–1568, <https://doi.org/10.1016/j.fusengdes.2015.11.021>. Proceedings of the 12th International Symposium on Fusion Nuclear Technology-12 (ISFNT-12)
- [27] T. Eade, M. Garcia, R. Garcia, F. Ogando, P. Pereslavtsev, J. Sanz, G. Stankunas, A. Travleev, Activation and decay heat analysis of the european demo blanket concepts, *Fusion Eng. Des.* 124 (2017) 1241–1245.
- [28] M. Sohal, M. Ebner, P. Sabharwal, P. Sharpe, Engineering database of liquid salt thermophysical and thermochemical properties, Idaho Natl. Lab. Idaho Falls CrossRef (2010).
- [29] A.C. Franken, J.A. Nolten, M.H. Mulder, D. Bargeman, C.A. Smolders, Wetting criteria for the applicability of membrane distillation, *J Memb Sci* 33 (3) (1987) 315–328, [https://doi.org/10.1016/S0376-7388\(00\)80288-4](https://doi.org/10.1016/S0376-7388(00)80288-4).
- [30] A. Inayat, B. Reinhardt, J. Herwig, C. Küster, H. Uhlig, S. Krenkel, E. Raedlein, D. Enke, Recent advances in the synthesis of hierarchically porous silica materials on the basis of porous glasses, *New J. Chem.* 40 (5) (2016) 4095–4114, <https://doi.org/10.1039/c5nj03591k>.
- [31] S. Flaischlen, G.D. Wehinger, Synthetic packed-bed generation for cfd simulations: Blender vs. star-ccm+, 2019.
- [32] A.V. Zhirkin, B.V. Kuteev, Three-dimensional model of DEMO-FNS facility considering neutronics and radiation shield problems, *Heliyon* 5 (5) (2019), <https://doi.org/10.1016/j.heliyon.2019.e01630>.
- [33] E. Achenbach, Heat and flow characteristics of packed beds, *Exp. Therm Fluid Sci.* 10 (1) (1995) 17–27, [https://doi.org/10.1016/0894-1777\(94\)00077-L](https://doi.org/10.1016/0894-1777(94)00077-L).
- [34] PED 2014/68/EU, Directive of the European Parliament and of the council of 15 May 2014 on the harmonisation of the laws of the Member States relating to the making available on the market of pressure equipment.
- [35] ESP Decree, Decree 99–1046 of 13/12/1999 on Pressure Equipment EN.
- [36] ESPN Order, French Order 30 December 2015 for Nuclear Pressure Equipment.
- [37] R. Muñoz, F.J. Calvo, S. Sádaba, A.M. Gil, J. Rodríguez, J. Vallory, M. Zmitko, Y. Poitevin, Analysis of test blanket module attachments under electromagnetic loads by using a dynamic amplification factor envelope, *Fusion Eng. Des.* 136 (2018) 1247–1251, <https://doi.org/10.1016/J.FUSENGDES.2018.04.110>.
- [38] RCC-MRx, Design and Construction Rules for Mechanical Components of Nuclear Installations.
- [39] J. Park, J. Yoon, J. Eoh, H. Kim, M. Kim, Optimization and sensitivity analysis of the nitrogen brayton cycle as a power conversion system for a sodium-cooled fast reactor, *Nucl. Eng. Des.* 340 (2018) 325–334, <https://doi.org/10.1016/j.nucengdes.2018.09.037>.
- [40] Hollomet, Hollomet - Hollow spheres, 2020.
- [41] M.S. Yim, F. Caron, Life cycle and management of carbon-14 from nuclear power generation, *Prog. Nucl. Energy* 48 (1) (2006) 2–36.
- [42] W.J. Davis, CARBON-14 PRODUCTION IN NUCLEAR REACTORS. Technical Report, 1977.
- [43] G.L. Khorasanov, A.P. Ivanov, A.I. Blokhin, Polonium issue in fast reactor lead coolants and one of the ways of its solution, International Conference on Nuclear Engineering, Proceedings, ICONE 2 (January) (2002) 711–717.
- [44] G. Hollenberg, B. Mastel, Helium bubbles in irradiated boron carbide (HEDL-SA–1675-FP) (1979).
- [45] A. Fierro, F. Sordo, I. Carbajal-Ramos, J. Perlado, A. Rivera, Conceptual design of a ceramic breeding blanket for laser fusion power plants with online tunable tritium breeding ratio based on a variable neutron reflector: remarkable no need of isotopic enrichment, *Fusion Eng. Des.* 155 (2020) 111648, <https://doi.org/10.1016/j.fusengdes.2020.111648>.